Zamfara International Journal of Sci. Tech. Educ. & Mathematics
The Official Journal of the Department of Science Education
Federal University Gusau, Zamfara State, Nigeria
Volume 2, Number 3, December, 2025
ISSN: 2251 – 0974

www.foefugusau.com.ng
des@fugusau.edu.ng
DOI: https://doi.org/10.64348/zije.2025204

Analysis of Aeromagnetic Data of North-Eastern Part of Sokoto Basin for Identification of Geological Structures in Sokoto State, Nigeria

ABDULRASHEED, Mohammed[1]
Email: bisalam2325@wufpbk.edu.ng
Tel.: 07062049929

ATIKU, Usman Kende[1]
atikuu31@gmail.com
Tel.: 08063699893

RILWANU, Bello[1]
rilwanbg@yahoo.com
Tel.: 08034246747

SHEHU, Umar[2]
umarshehu140@yahoo.com
Tel.: 08034576601

ABUBAKAR, Samaila[2]
Email: abunaamore1@gmail.com
Tel.: 08065259951

[1]Department of Science Technology, Waziri Umaru Federal Polytechnic Birnin Kebbi, Kebbi State, Nigeria.
[2]Department of Science Education, Waziri Umaru Federal Polytechnic Birnin Kebbi, Kebbi State, Nigeria.

Abstract

This study centers on investigating the subsurface condition of the north-eastern part of the Sokoto Basin using aeromagnetic data for geological structures. This area falls within the Sokoto Basin, the Nigerian portion of the Iullemmeden Basin, and covers four adjacent quarter-degree sheets of Gada, Sabon Birnin, Rabah, and Isa. Qualitative and quantitative interpretation techniques which include First and Second Vertical Derivatives, Upward Continuation, Analytic Signal, Source Parameter Imaging, and Euler Deconvolution were employed. The first and second vertical derivatives applied show the response of the target structures, which helps to remove noise caused by high-frequency shallow anomalies. The analytic signal map shows high analytic signal amplitude most prominently around the east-west flank, with low analytic signal value towards the centre, with amplitude ranging from 0.00 nT to 0.08 nT. The data was subjected to upward continuation at 2 km, 5 km, 10 km, and 15 km with magnetic field values ranging from 7.25 nT to 84.27 nT, 17.73 nT to 74.46 nT, 22.17 nT to 68.86 nT, and 23.83 nT to 67.12 nT, respectively. The result shows the magnetic anomaly for deep-seated features becomes more obvious by projecting from a lower elevation to a higher elevation, thereby removing noise caused by high-frequency shallow anomalies.

Key words: Geological structures, Aeromagnetic data, Sokoto basin, Iullemmeden basin.

Introduction

The contents of the Earth have long been of concern to mankind. Man has tried to unravel its complexity and delve into its origin through various geophysical methods. Particularly the subsurface has been of great concern to geoscientists, who seek to investigate it using diverse means, some for the purpose of knowledge, while others do it for the exploration of economic resources such as minerals and hydrocarbons. Economic minerals, such as oil, gas, and groundwater lie concealed

Zamfara International Journal of Sci. Tech. Educ. & Mathematics
The Official Journal of the Department of Science Education
Federal University Gusau, Zamfara State, Nigeria
Volume 2, Number 3, December, 2025
ISSN: 2251 – 0974

www.foefugusau.com.ng
des@fugusau.edu.ng
DOI: https://doi.org/10.64348/zije.2025204

beneath the earth's surface, thus hidden from direct view (Bonde *et al.*, 2014). Depth to basement is a germane exploration parameter particularly for areas where there may be mature hydrocarbons. Geologists and Geophysicists have done extensive work in terms of geological mapping of Nigeria. They have worked on the interpretation of aeromagnetic data obtained mainly from restricted areas of their studies (Emujakporue and Ofoha, 2015). Depth to anomalous magnetic source interpretation provides a clue to the sedimentary basin architecture for hydrocarbon exploration as well as the presence of minerals (Onyewuchi and Ugwu, 2017). The magnetic method is one of the oldest geophysical techniques used to delineate subsurface structures and determine the source of specific anomalies present in an area under investigation (Reeves, 2007). Minerals are of importance to the economy of a nation if discovered and harnessed. As this will create a productive environment for business opportunities, boost the nation's economy, and provide raw materials for industrial uses which might in turn reduce the level of unemployment, thereby eradicating poverty in the country. It is therefore necessary to carry out research of this magnitude using high-resolution aeromagnetic (HRAM) data. Exploitation of mineral resources has assumed prime importance in several developing countries including Nigeria. Nigeria is endowed with abundant mineral resources, which have contributed immensely to the national wealth with associated socio-economic benefits. Mineral resources are an important source of wealth for a nation but before they are harnessed, they have to pass through the stages of exploration, mining, and processing (Adewumi and Salako, 2017).

In a related development, Mukhtar and Congjiao (2012) stated that Nigeria has seven (7) basins in which active exploration activities can be carried out and these basins include the following; Anambra Basin, Benue Trough, Benin Basin, Bida Basin, Bornu Basin, Niger Delta Basin, and Sokoto Basin.

Objective of the Study

The objective of this study is to analyze aeromagnetic data from the north-eastern part of the Sokoto Basin to identify geological structures, such as faults, fractures, and lineaments that may be indicatives of mineralization.

Research Question

1. What are the dominants structural trends and lineaments in the north-eastern part of the Sokoto Basin?
2. Can aeromagnetic data be used to identify potential mineralized zones in the study area?

Research Hypotheses

1. The north-eastern part of the Sokoto Basin has significant geological structures, such as faults and fractures that are indicative of mineralization.
2. Aeromagnetic data can be used to identify and characterize these geological structures, providing valuable insights for further exploration and research.

Location of the Study Area

This study area lies between longitude 005˚ E to 006˚ E and latitude 13˚ 00' N to 13.5˚N. It is made up of four (4) sheets which include; Gada (sheet 4), Sabon Birnin (sheet 5), Rabah (sheet 11), and Isa (sheet 12) respectively. The Sokoto sedimentary basin is located in the North-Western part of Nigeria; it is situated along the longitude 3˚ 30' E to 7˚ 00' E and latitude 10˚ 30' N to 14˚ 00' N, with an approximate area of 59,570 km². The Sokoto Basin is also known as the Iullemmeden Basin, with an average elevation varying from 250 m to 400 m above sea level (Ofoha *et al.*, 2016).

Zamfara International Journal of Sci. Tech. Educ. & Mathematics
The Official Journal of the Department of Science Education
Federal University Gusau, Zamfara State, Nigeria
Volume 2, Number 3, December, 2025
ISSN: 2251 – 0974

www.foefugusau.com.ng
des@fugusau.edu.ng
DOI: https://doi.org/10.64348/zije.2025204

Materials and Methods

Materials

The software and data used in the course of this research work include various geophysical software such as Geosoft Oasis Montaj (v7.2), Golden Software Surfer 13, Golden Software Grapher 8, and MATLAB. The aeromagnetic d ata was acquired from the Nigerian Geological Survey Agency (NGSA).

Methods

As the aircraft flies, the magnetometer records tiny variations in the intensity of the ambient magnetic field due to the temporal effects of the constantly varying solar wind and spatial variations in the Earth's magnetic field, the latter being due both to the regional magnetic field and the local effect of magnetic minerals in the Earth's crust. By subtracting the solar and regional effects, the resulting aeromagnetic map shows the spatial distribution and relative abundance of magnetic minerals (most commonly the iron oxide mineral magnetite) in the upper levels of the crust. Because different rock types differ in their content of magnetic minerals, the magnetic map allows a visualization of the geological features of the upper crust in the subsurface, particularly the spatial geometry of bodies of rock and the presence of structures such as faults and folds. The raw total magnetic intensity data acquired from the Nigerian Geological Survey Agency was processed using Golden Software Surfer and Geosoft Oasis Montaj. The acquired total magnetic intensity data was converted into a grid file and imported into the Oasis Montaj database for processing. Enhancement of magnetic data is very important in the study of structural features because it enhances the edges of anomalies. The first vertical derivative, second vertical derivative, and analytical signal were used in this research to enhance the upward continued field data. Enhanced potential field anomalies are primarily used in qualitative visual analysis to infer the approximate shape and orientations of anomalous sources of interest which may be localized features at relatively shallow depths, or large-scale structures at greater depth (Sharma, 2002).

Detection of the edges of geological structures from the analysis of potential field data is commonly performed. The horizontal gradient of a field φ sampled at locations Δx intervals along a profile may be calculated in the space domain as:

$$\frac{d\varphi}{dx} = \frac{\varphi_{x+\Delta x} - \varphi}{\Delta x}, \qquad 1$$

or in the frequency domain (Gunn, 1975)

$$A'(f) = A(f)(if)^n \qquad 2$$

where A(f) is the amplitude at a frequency f, i is the complex number and n is the order of the derivative. The gradient profiles, being narrower in width, clearly show the body location more precisely than do the original data, but since derivatives are high-pass filters they also amplify any noise present in the data.

Vertical Derivative Filters

The vertical derivative is applied to total magnetic field data to enhance the most shallow geological sources and it can be calculated in either the space or the frequency domain. The enhancement sharpens anomalies over bodies and tends to reduce their complexity, allowing a clearer imaging of a causing structure. The transformation can be noisy since it will amplify short-wavelength noise. Vertical gradients of potential fields are also a mainstay of the interpretation process, principally because they sharpen the response of geophysical features. This filtering method is effective in

Zamfara International Journal of Sci. Tech. Educ. & Mathematics
The Official Journal of the Department of Science Education
Federal University Gusau, Zamfara State, Nigeria
Volume 2, Number 3, December, 2025
ISSN: 2251 – 0974

www.foefugusau.com.ng
des@fugusau.edu.ng
DOI: https://doi.org/10.64348/zije.2025204

enhancing anomalies due to shallow sources; it narrows the width of anomalies and is also very effective in locating source bodies more accurately (Cooper and Cowan, 2004). In the frequency domain, they can be calculated using (Gunn, 1975):

$$A'(f) = A(f)|f|^n \quad 3$$

where A(f) is the amplitude at a frequency f, and n is the order of the derivative.

Vertical derivatives are a measure of curvature, and large curvatures are associated with shallow anomalies. Thus, it enhances near-surface features at the expense of deeper anomalies. The first and second vertical derivatives (FVD & SVD) are given as:

$$FVD = \frac{\partial M}{\partial z} \quad , \quad SVD = \frac{\partial^2 M}{\partial z^2} \quad 4$$

where M is the potential field anomaly.

The second vertical gradient can be calculated by exploiting Laplace's equation below: (Blakely, 1995)

$$\frac{\partial^2 \varphi}{\partial z^2} = -\frac{\partial^2 \varphi}{\partial x^2} - \frac{\partial^2 \varphi}{\partial y^2} \quad 5$$

The first vertical derivative is an important step in the interpretation of aeromagnetic data, particularly in studies dealing with narrow and shallow anomalies. It reduces the effect of long-wavelength regional anomalies (which are usually deeper) and enhances the higher frequency shallow anomalies (Milligan and Gunn, 1997).

Second vertical derivative filters are used to enhance subtle anomalies while reducing regional trends. These filters are considered most useful for defining the edges of bodies and for amplifying fault trends. In mathematical terms, a vertical derivative can be shown to be a measure of the curvature of the potential field, while zero values (or contours) of second vertical derivative contours define the edge of the causative body (Telford et al., 1990). Thus, the second vertical derivative is in effect a measure of the curvature, i.e., the rate of change of non-linear magnetic gradients. The zero magnetic contours of the second vertical derivative often coincide with lithological boundaries (Blakely, 1995).

Upward Continuation of Residual Field

This is a mathematical technique that projects data taken at an elevation to a higher elevation. It is a filtering technique that removes noise caused by high-frequency (short wavelength) anomalies which usually arise from near-surface cultural features in the survey area. It accentuates anomalies caused by deep sources at the expense of anomalies caused by shallow sources (Mekonnen, 2004). The upward continued ΔF (the total field magnetic anomaly) at a higher level (z = -h) is given by:

$$\Delta F\,(x, y, -h) = \frac{h}{2\pi} \iint \frac{\Delta F(x,y,0)\,dx\,dy}{((x-x_0)^2+(y-y_0)^2+h^2)} \quad 6$$

The empirical formula gives the field at an elevation h above the plane of the observed field (z = 0) in terms of the average value ΔF at the point (x, y, 0). Generally, deep-seated magnetic sources are considered to have a low spatial frequency equivalent to large lateral extent or long wavelengths and broad anomalies; while near-surface or shallow magnetic sources result in a high spatial frequency corresponding to short lateral distance or short wavelength and narrow anomalies (Dobrin, 1976).

The Analytic Signal Technique

This is a filter applied to magnetic data aimed at simplifying the fact that magnetic bodies usually have a positive and negative peak associated with them, which in many cases makes it difficult to determine the exact location of the causative body. The analytic signal is a complex function formed

Zamfara International Journal of Sci. Tech. Educ. & Mathematics
The Official Journal of the Department of Science Education
Federal University Gusau, Zamfara State, Nigeria
Volume 2, Number 3, December, 2025
ISSN: 2251 – 0974

www.foefugusau.com.ng
des@fugusau.edu.ng
DOI: https://doi.org/10.64348/zije.2025204

through a combination of the horizontal and vertical derivatives of the magnetic anomaly. In 3D, the analytic signal of the magnetic anomaly field T is defined as:

$$A(x, y, z) = \frac{\partial T}{\partial x}\hat{x} + \frac{\partial T}{\partial y}\hat{y} + i\frac{\partial T}{\partial z}\hat{z} \qquad 7$$

where $\hat{x}$, $\hat{y}$ and $\hat{z}$ are unit vectors in the x, y and z directions, respectively, $\frac{\partial T}{\partial z}$ is the vertical derivative of the magnetic anomaly field intensity, $\frac{\partial T}{\partial x}$ and $\frac{\partial T}{\partial y}$ are the horizontal derivatives of the magnetic anomaly field intensity (Blakely, 1995).

The amplitude of the analytic signal in 3D is given by:

$$|[A(x, y, z)]| = \sqrt{\left(\frac{\partial T}{\partial x}\right)^2 + \left(\frac{\partial T}{\partial y}\right)^2 + \left(\frac{\partial T}{\partial z}\right)^2} \qquad 8$$

Expression of the amplitude of the analytic signal gives a function that produces maxima approximately over the edges of the magnetic body source. Their results showed that the location of the analytic signal depends on depth. When the prism is at shallow depth the locations of the maxima are essentially over both edges of the prism. The locations become shifted from edges when the top depth increases. In the 2D case, only for an infinitely thin dike and infinitely vertical step or contact, the locations of the 2D analytic signal's maxima are directly over the top surface edges of the causative body. However, for a vertical thin dike, the analytic signal's maxima are also offset away from both edges. In 3D and in general, the analytic signal amplitude is dependent on: the burial depth, extent and dipping angle of a source body, body's magnetization direction, and earth's magnetic field direction. For 2D magnetic sources, the analytic signal amplitude becomes independent of the magnetization direction.

Source Parameter Imaging (SPI)

This method makes the task of interpreting data significantly easier as shown by the SP Images generated from the residual field data. The colour legend in the SPI shows various colours that represent the depth estimates to magnetic source rock/body within the study area. This method utilizes the relationship between source depth and the local wavenumber (k) of the observed field, which can be calculated for any point within a grid of data through horizontal and vertical gradients. At peaks in the local wavenumber grid, the source depth is equal to n/k, where n depends on the assumed source geometry (analogous to the structural index in Euler deconvolution); for example, n = 1 for a contact, n = 2 for a dyke (Blakely and Simpson, 1986). The assumed geometry for each magnetic body was used to determine the area where we have shallow and deep-lying magnetic bodies in the study area. Peaks in the wavenumber grid were identified using a peak tracking algorithm and valid depth estimates were also isolated. The source parameter imaging method was also employed in this work to estimate the depth from the local wavenumber of the analytical signal. The analytical signal A(x, z) is given as (Biswas *et al.*, 2017):

Zamfara International Journal of Sci. Tech. Educ. & Mathematics
The Official Journal of the Department of Science Education
Federal University Gusau, Zamfara State, Nigeria
Volume 2, Number 3, December, 2025
ISSN: 2251 – 0974

www.foefugusau.com.ng
des@fugusau.edu.ng
DOI: https://doi.org/10.64348/zije.2025204

$$A_1(x, z) = \frac{\partial m}{\partial y}(x, z) - j\frac{\partial m}{\partial x}(x, z) \quad 9$$

Where m (x, z) is the magnitude of the anomalous total magnetic field, j is the imaginary number, while x and z are Cartesian coordinates for the vertical and horizontal directions, respectively.

Euler Deconvolution

Any function *f (x, y, z)* is homogeneous of degree n if

$$f(tx, ty, tz) = t^n f(x, y, z) \quad 10$$

Where t is a real number. The plane of observation is taken at plane z = 0 and positive downward. Moreover, if *f* (*x, y, z*) is homogeneous of degree *n,* according to Thompson (1982) the following equation holds:

$$x\frac{\partial f}{\partial x} + y\frac{\partial f}{\partial y} + z\frac{\partial f}{\partial z} = nf \quad 11$$

This partial differential equation is known as Euler's homogeneity equation. Now, consider the total magnetic intensity of a point source located at the point (x_o, y_o, z_o) relative to the point of observation (*x, y, z*):

$$\Delta T(x, y) = f[(x - x_o), (y - y_o), (z - z_o)] \quad 12$$

The above equation can be written as:

$$(x - x_o)\frac{\partial \Delta T}{\partial x} + (y - y_o)\frac{\partial \Delta T}{\partial y} + (z - z_o)\frac{\partial \Delta T}{\partial z} = n\Delta T \quad 13$$

This equation expresses the magnetic field strength at any point in terms of the gradients of the total magnetic field. These gradients are related to different magnetic sources by the structural index, N. The structural index N is a measure of the rate of change of distance of a field (Reid *et al.*, 1990). Thompson, (1982) gives more detailed discussion on the degree of homogeneity of potential fields and structural indices of Euler deconvolution.

Presentation of Results and Discussion

The results of First Vertical Derivative (FVD), Second Vertical Derivative (SVD), Upward Continuation, Analytical Signal Technique, Source Parameter Imaging (SPI), and Euler Deconvolution Technique are shown in Figure 1, Figure 2, Figure 3 (a, b, c, & d), Figure 4, Figure 5, and Figure 6 respectively.

Zamfara International Journal of Sci. Tech. Educ. & Mathematics
The Official Journal of the Department of Science Education
Federal University Gusau, Zamfara State, Nigeria
Volume 2, Number 3, December, 2025
ISSN: 2251 – 0974

www.foefugusau.com.ng
des@fugusau.edu.ng
DOI: https://doi.org/10.64348/zije.2025204

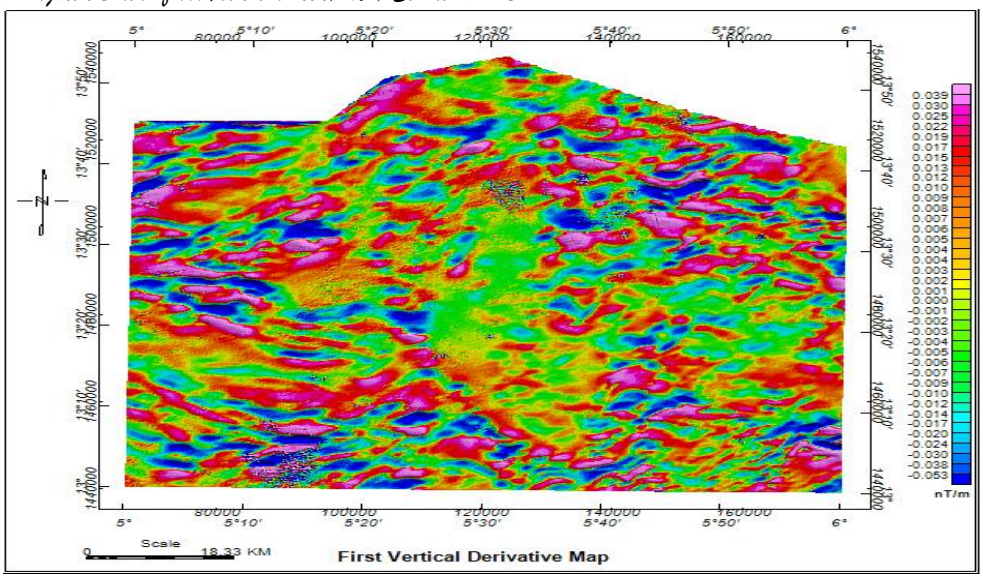

Figure 1: First Vertical Derivative Map

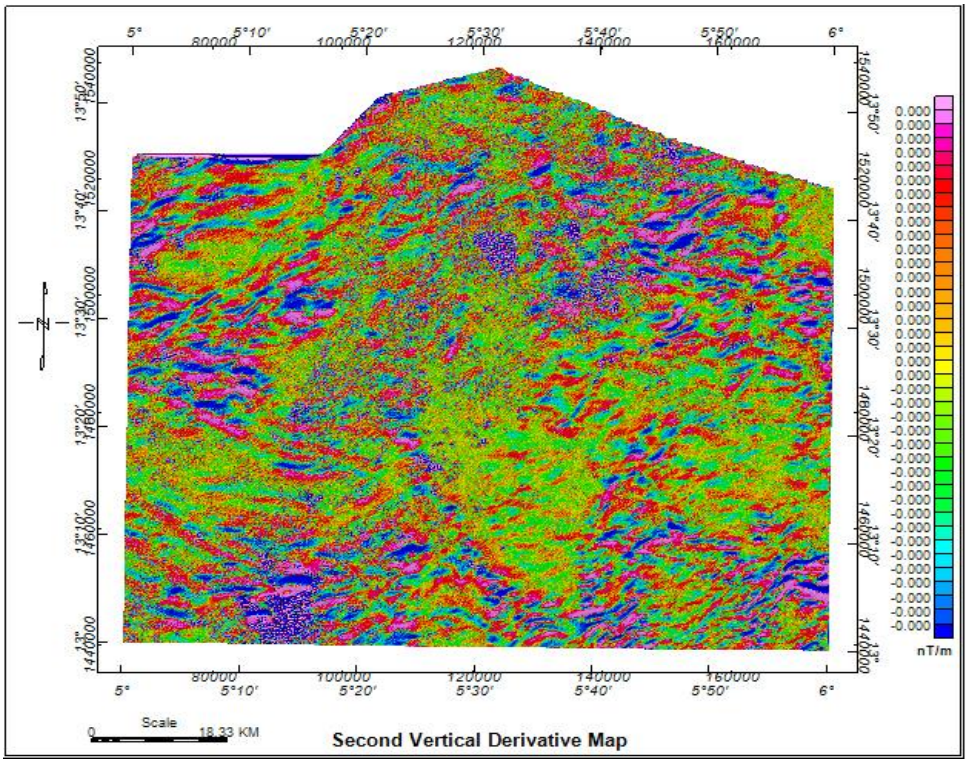

Zamfara International Journal of Sci. Tech. Educ. & Mathematics
The Official Journal of the Department of Science Education
Federal University Gusau, Zamfara State, Nigeria
Volume 2, Number 3, December, 2025
ISSN: 2251 – 0974

www.foefugusau.com.ng
des@fugusau.edu.ng
DOI: https://doi.org/10.64348/zije.2025204

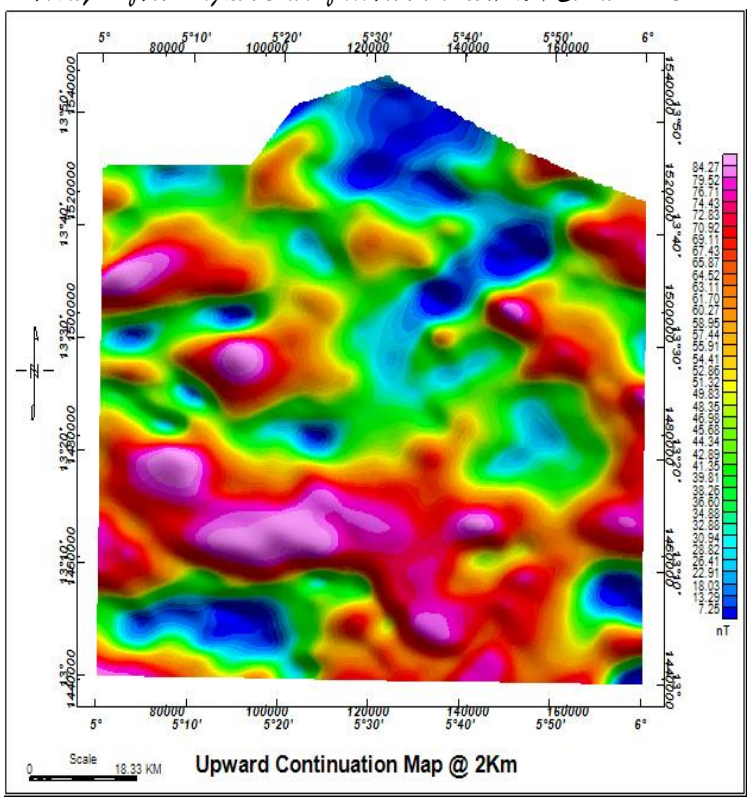

Figure 3a: Upward Continuation Map @ 2 km

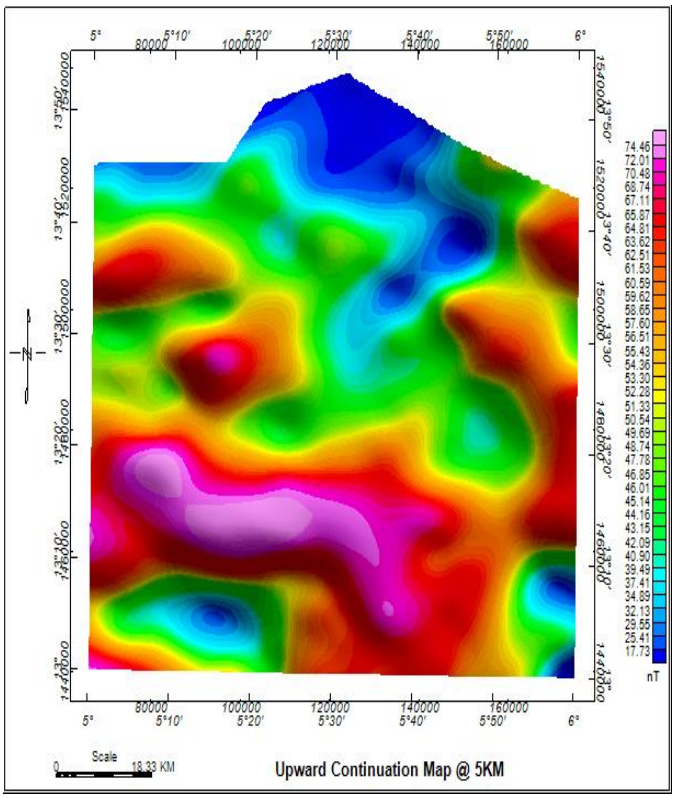

Figure 3b: Upward Continuation Map @ 5 km

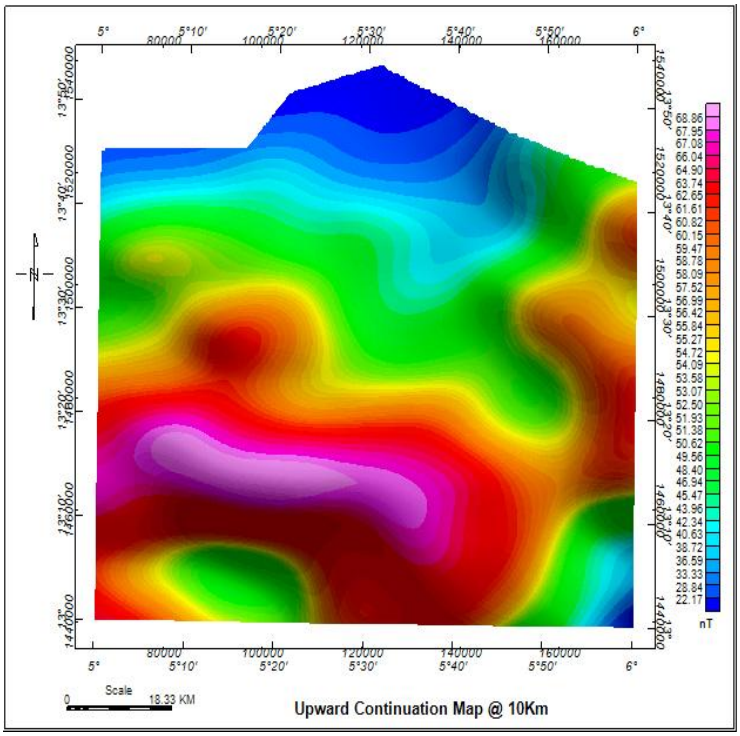

Figure 3c: Upward Continuation Map @ 10 km

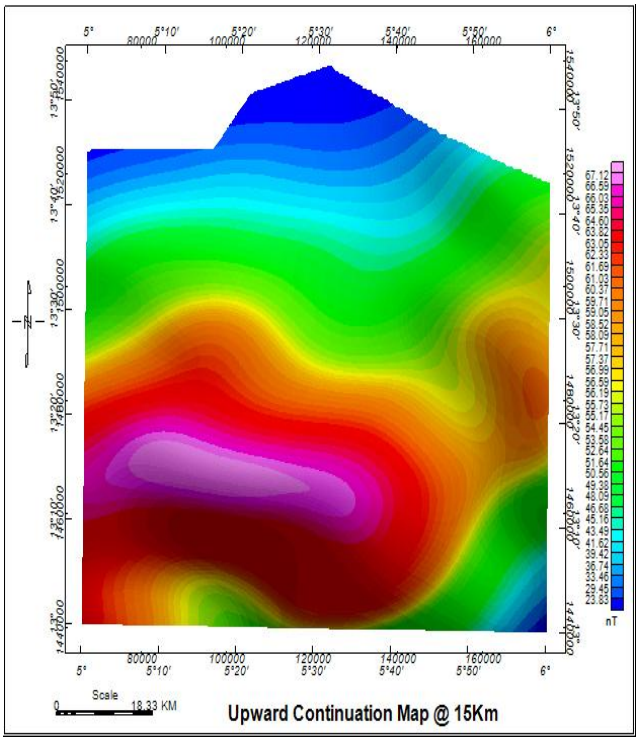

Figure 3d: Upward Continuation Map @ 15km

Zamfara International Journal of Sci. Tech. Educ. & Mathematics
The Official Journal of the Department of Science Education
Federal University Gusau, Zamfara State, Nigeria
Volume 2, Number 3, December, 2025
ISSN: 2251 – 0974

www.foefugusau.com.ng
des@fugusau.edu.ng
DOI: https://doi.org/10.64348/zije.2025204

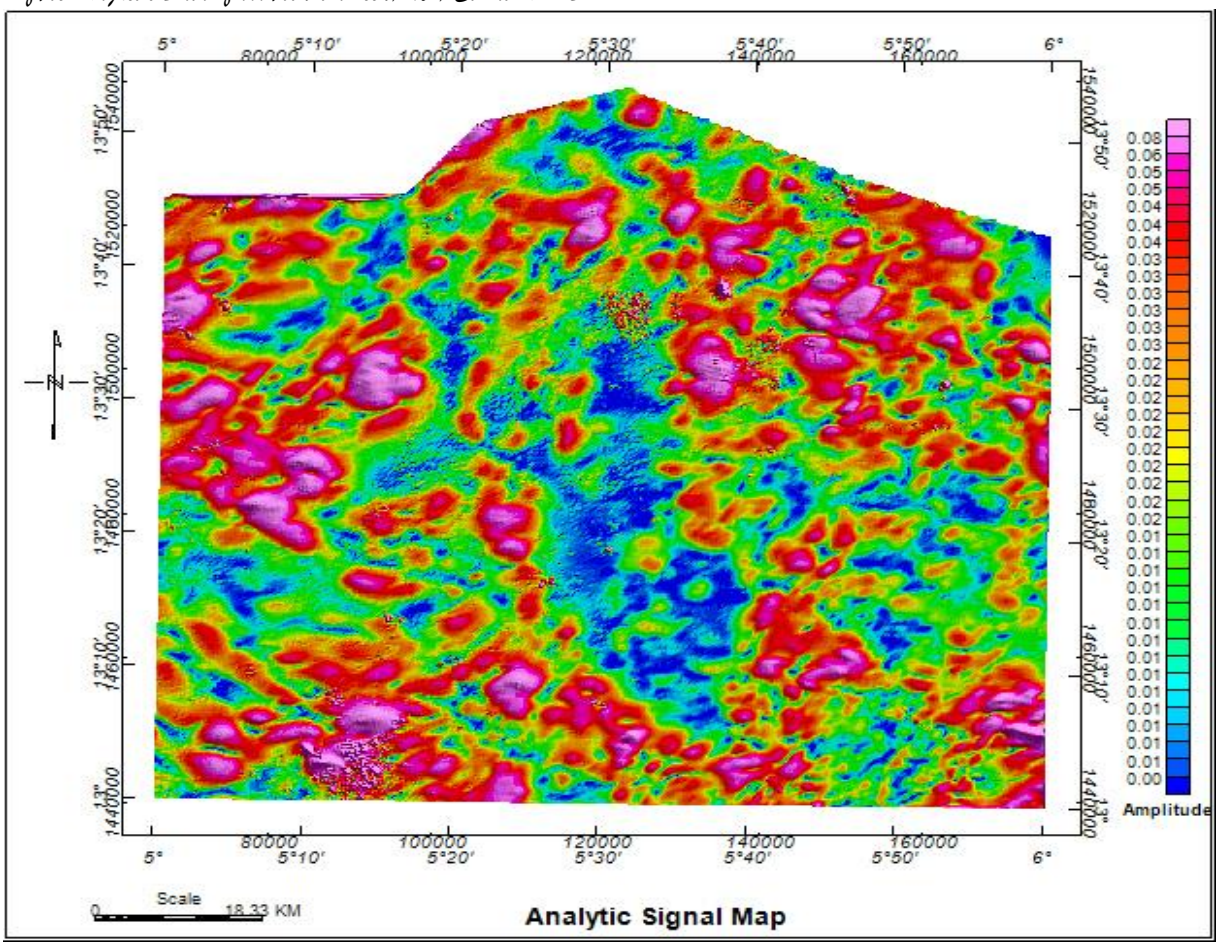

Figure 4: Analytic Signal Map

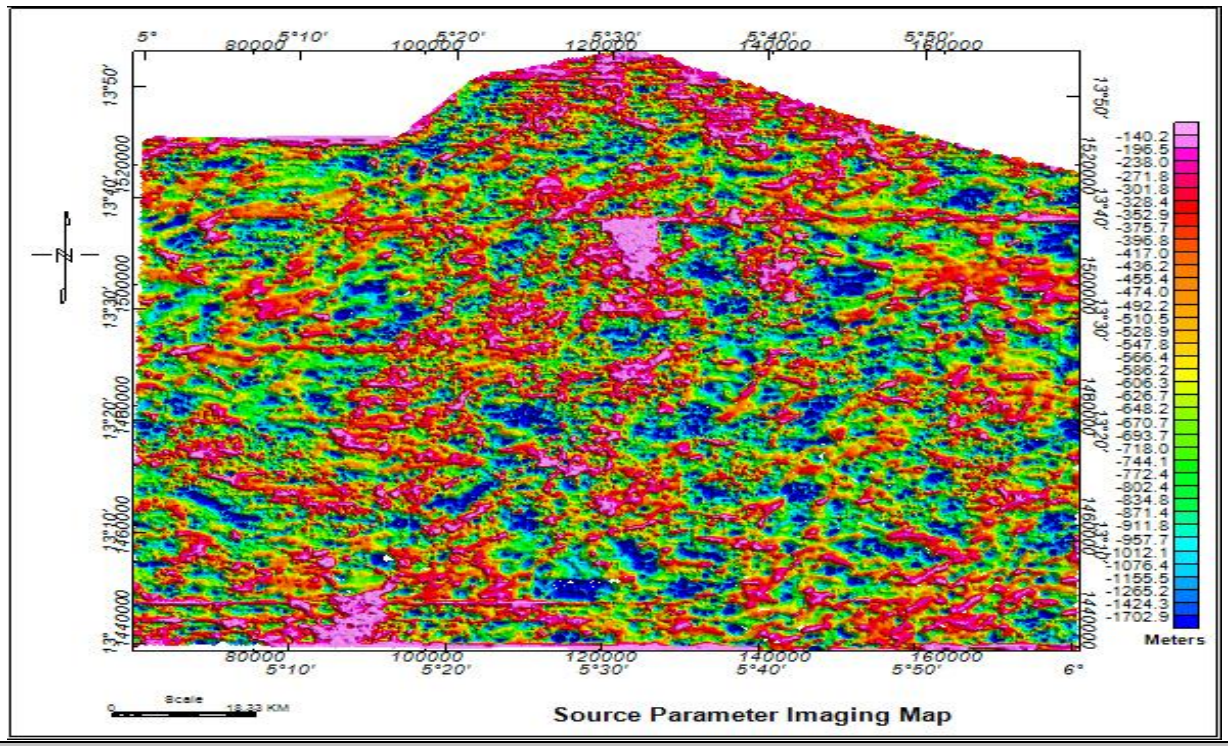

Zamfara International Journal of Sci. Tech. Educ. & Mathematics
The Official Journal of the Department of Science Education
Federal University Gusau, Zamfara State, Nigeria
Volume 2, Number 3, December, 2025
ISSN: 2251 – 0974

www.foefugusau.com.ng
des@fugusau.edu.ng
DOI: https://doi.org/10.64348/zije.2025204

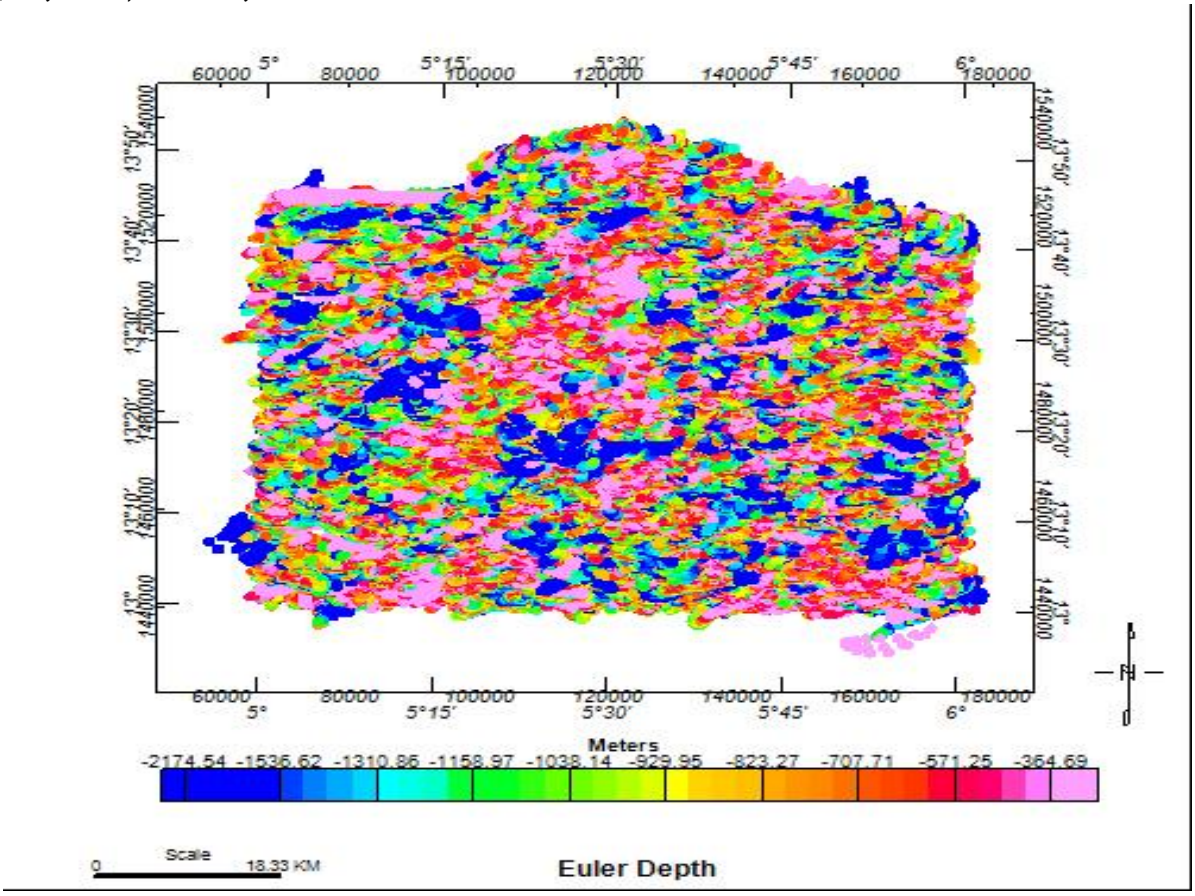

Figure 6: Euler Depth

Figure 1: First Vertical Derivative (FVD) Map. The map shows the response of the target structures, which helps remove noise caused by high-frequency shallow anomalies, with magnetic field values ranging from -0.053 nT/m to 0.039 nT/m. Several linear highs (red) and lows (blue) are evident, trending predominantly in the NE-SW and NW-SE directions. These linear features are interpreted as fault lines or shear zones within the basement complex, which likely influence the overlying sedimentary architecture.

Figure 2: Second Vertical Derivative (SVD) Map. The map shows a more enhanced view of near-surface anomalies than the FVD map, with magnetic field values ranging from -0.053 nT/m to 0.039 nT/m. It provides a much clearer view of the edges of anomalies because it sharpens them. The SVD analysis effectively discriminates local features while suppressing broad regional structures. The zero contours of the SVD (white lines) clearly delineate the boundaries of magnetic source bodies, which often correspond to lithological contacts or faults. The NE-SW structural trend remains dominant.

Figure 3: Upward Continuation Maps. (a) 2 km, (b) 5 km, (c) 10 km, (d) 15 km. The appropriation of the magnetic intensities from deeper structures led to applying the upward-continued filter to suppress the effects of shallow anomalies. The RMI grid was continued to 15 km to see deeper signatures coming from deeper structures. This helped smooth out high-frequency anomalies relative to low-frequency anomalies.

Figure 3a (2 km): Magnetic field values range from 7.25 nT to 84.27 nT. Shallow, high-frequency anomalies are still prominent.

Zamfara International Journal of Sci. Tech. Educ. & Mathematics
The Official Journal of the Department of Science Education
Federal University Gusau, Zamfara State, Nigeria
Volume 2, Number 3, December, 2025
ISSN: 2251 – 0974

www.foefugusau.com.ng
des@fugusau.edu.ng
DOI: https://doi.org/10.64348/zije.2025204

Figure 3b (5 km): Magnetic field values range from 17.73 nT to 74.46 nT. Regional trends begin to emerge as shallow features are attenuated.

Figure 3c (10 km): Magnetic field values range from 22.17 nT to 68.86 nT. A broad, high-amplitude anomaly in the central-southern part of the study area becomes clearly visible, suggesting a deep-seated magnetic source body.

Figure 3d (15 km): Magnetic field values range from 23.83 nT to 67.12 nT. The deep-seated anomaly persists, confirming its origin from a profound depth within the basement. These maps show the magnetic anomaly for deep-seated features more obviously by projecting field data from a lower elevation to a higher elevation.

Figure 4: Analytic Signal Amplitude Map. The map shows the analytic signal amplitude at various locations, ranging from 0.00 nT to 0.08 nT. The map shows high analytic signal amplitude (red and yellow) most prominently around the east-west flanks, with low analytic signal values (blue) towards the centre. Since the analytical amplitude is independent of magnetization direction, the high amplitudes directly indicate the locations of sharp magnetic contrasts, such as the edges of intrusive bodies, faults, or basement highs. The arcuate pattern of high amplitudes along the flanks suggests a possible basin-bounding fault system, while the central low may represent a deeper, less disturbed sedimentary section.

Figure 5: Source Parameter Imaging (SPI) Depth Estimate Map. The colour legend shows the depth estimate to the magnetic source (sediment/basement interface). The depth varies between 0.14 km and 1.7 km. The greatest sediment thickness (deepest basement) is found in the south-central to north-eastern part, which is in agreement with the work of Ofoha *et al.* (2016). However, relatively deeper areas are also scattered around the northern and southern parts. This analysis helps in edge detection, with various anomalous bodies following the trend of the residual anomalies. The SPI map effectively outlines the topography of the basement surface, showing areas prospective for deeper sedimentary accumulation.

Figure 6: Euler Deconvolution Depth Solutions. The plot shows depth solutions clustered around regions where geological structures are located. The depth solutions (calculated for a structural index appropriate for geologic contacts) have a range of approximately -0.35 km to -2.17 km (negative denoting depth below the datum). These depth values correspond to the probable locations and depths of the magnetic bodies (primarily the basement surface) in the study area. The clustering of solutions along linear trends (e.g., NE-SW) provides a quantitative confirmation of the fault systems inferred from the derivative maps. The average depth range indicates the presence of predominantly shallow-to-moderate depth features.

Synthesis of Interpretation: The integrated analysis reveals a structurally complex basement underlying the north-eastern Sokoto Basin. The dominant NE-SW and subsidiary NW-SE structural trends, identified as faults and shear zones from derivative maps and Euler solutions, compartmentalize the basin. The SPI and Euler depth estimates consistently show a basement depth generally less than 2 km, with the deepest section (~1.7 km) located in the south-central to north-eastern region. The analytic signal and upward continuation confirm the presence of deep-seated magnetic sources influencing the regional magnetic signature. This structural framework is crucial for understanding basin evolution and identifying zones where these structures might have created traps or pathways for hydrocarbons or mineralized fluids.

Conclusion

The aeromagnetic data proved valuable in the delineation of subsurface structures and estimation of basement depth in the north-eastern Sokoto Basin. The application of both qualitative and

Zamfara International Journal of Sci. Tech. Educ. & Mathematics
The Official Journal of the Department of Science Education
Federal University Gusau, Zamfara State, Nigeria
Volume 2, Number 3, December, 2025
ISSN: 2251 – 0974

www.foefugusau.com.ng
des@fugusau.edu.ng
DOI: https://doi.org/10.64348/zije.2025204

quantitative techniques successfully revealed a dominant NE-SW structural trend, interpreted as fault systems, and delineated the configuration of the basement topography. The sediment thickness, estimated to reach up to 1.7 km, indicates that the sediments are sufficiently deep to have undergone maturation processes if organic-rich source rocks are present. The integration of all methods provides a coherent geological model of the area, highlighting zones of structural complexity that are primary targets for further exploration for mineral and hydrocarbon resources.

Recommendation

Based on the findings of this study, the following recommendations are made:

1. Ground Truthing: The inferred fault systems and depth estimates should be verified with other geophysical methods, such as seismic reflection surveying or magnetotellurics, to better characterize the structures and basin geometry.
2. Detailed Geochemical Studies: Areas with identified structural features (faults, basement highs) should be investigated with detailed soil gas geochemistry or gravity surveys to assess their potential for hydrocarbon accumulation or mineral concentration.
3. Integration with Geological Data: The results of this study should be integrated with existing geological maps, well log data, and borehole information from the basin to build a more robust and calibrated geological model

Acknowledgements

To Nigeria Geological Survey Agency (NGSA), thank you for releasing the data for us at a subsidized rate for the purpose of this research work.

References

Adewumi, T. & Salako, K. A. (2017). Delineation of mineral potential zone using high resolution aeromagnetic data over part of Nasarawa State, North Central, Nigerial. *Egypt. J. Petrol. (2017).* https://doi.org/10.1016/j.ejpe.2017.11.002.

Biswas, A., Parija, M. P. & Kumar, S. (2017). Global nonlinear optimization for the interpretation of source parameters from total gradient of gravity and magnetic anomalies caused by thin dyke. Ann. Geophys. 60(2):G0218.

Blakely, R. J. (1995). Potential Theory in Gravity and Magnetic Applications. 1st Ed. Cambridge, UK: Cambridge University Press;

Blakely, R. J. & Simpson, R. W. (1986). Approximating edges of source bodies from magnetic or gravity anomalies. *Geophysics*, 51: 1494 – 1498.

Bonde, D. S., Udensi, E. E. & Rai, J. K. (2014). Spectral Depth Analysis of Sokoto Basin. *Journal of Applied Physics (IOSR-JAP),* Volume 6, PP 15-21.

Cooper, G. R. J. & Cowan, D. R. (2004). Filtering using variable order vertical derivatives: *Journal of computer and Geoscience* Vol. 30(5): 455-459.

Dobrin, M. B. (1976). Introduction to Geophysical Prospecting.Mc-Graw Hill Books Co (3rd Ed.)N.Y.Pp. 630.

Emujakporue, G. & Ofoha, C. C. (2015). Spectral Depth Estimate of subsurface Structures over Parts of Offshore Niger Delta, Nigeria. *The International Journal of Engineering and Science (IJES),* 4(10): 42-53.

Gunn, P. J. (*1975*). Linear Transformation of Gravity and Magnetic Fields. *Geophysical Prospecting,* 23, 300-312.

Mekonnen, T. K. (2004). Interpretation and Geodatabase of Dukes using Aeromagnetic data of Zimbabwe and Mozambique. *International Institute for Geoinformation science and Earth Observation, Enschede, the Netherlands*. Retrieved from http://www.slideserve.com/phila/partners.

Milligan ,& Gunn (1997). *Enhancement and presentation of geophysical data* P. R.

Zamfara International Journal of Sci. Tech. Educ. & Mathematics
The Official Journal of the Department of Science Education
Federal University Gusau, Zamfara State, Nigeria
Volume 2, Number 3, December, 2025
ISSN: 2251 – 0974

www.foefugusau.com.ng
des@fugusau.edu.ng
DOI: https://doi.org/10.64348/zije.2025204

Mukhtar H. & Congjiao, X. (2012). Nigeria's inland basins: Investment opportunities and environment. *Journal of Petroleum and Gas Exploration Research.* Vol. 2(11): 202-211.

Ofoha, C. C., Emujakporue, G., Ngwueke, M. I. & Kiani, I. (2016). Determination of Magnetic Basement Depth over Parts of Sokoto Basin, within Northern Nigeria, Using Improved Source Parameter Imaging (ISPI) Technique. *World Scientific News.* 50, 266-277.

Onyewuchi, R. A. & Ugwu, S. A. (2017). Geological Interpretation of the High Resolution Aeromagnetic Data over Okigwe-Udi Area, Anambra Basin, Nigeria, Using 3-D Euler Deconvolution and 2-D Spectral Inversion Methods. *Journal of Geography, Environment and Earth Science International* 10(1): 1-22.

Reid, A. B., J. M. Allsop, H., Granser, A. J. Millett. & I. W. Somerton. (1990). Magnetic interpretation in three dimensions using Euler deconvolution. Geophysics, 55, 80-90.

Revees, C. (2007). Aeromagnetic Surveys: principle, practice and interpretation. *Geosoft* INC.

Sharma, P. V. (2002). *Environmental and Engineering Geophysics.* Cambridge University Press, United Kingdom. 32, 221.

Telford, W. M., Geldard, L. P., Sherriff, R. E. Keys, & D. A. (1990). *Applied Geophysics* 2nd edition, Cambridge University Press, Cambridge, GB, 860 p.

Thomson, D. T. (1982). EULDPTH: A new technique for making computer-assisted depth estimates from magnetic data: *Geophysics*, 47; 31–37.